

Fan Acoustic Signatures in an Anechoic Wind Tunnel

Donald A. Dietrich,* Marcus F. Heidmann,† and John M. Abbott*
NASA Lewis Research Center, Cleveland, Ohio

One-third octave band and narrowband spectra and continuous directivity patterns radiated from an inlet are presented over ranges of fan operating conditions, tunnel velocity, and angle of attack. Compared to the tunnel static condition, tunnel flow markedly reduced the unsteadiness and level of the blade passage tone, revealed the cutoff design feature of the blade passage tone, and exposed a lobular directivity pattern for the second harmonic tone. The effects of tunnel flow are shown to be complete above a tunnel velocity of 20 m/sec. The acoustic signatures are also shown to be strongly affected by fan rotational speed, fan blade loading, and inlet angle of attack.

Introduction

THE inability of ground-static acoustic tests to yield turbofan engine fan acoustic characteristics indicative of that which would be measured during flight is well documented. Inflow disturbances present during static tests and absent under flight conditions interact with the rotor to generate tone and broadband noise not present during flight.¹⁻⁷ This noise resulting from the rotor interacting with inflow disturbances tends to mask the benefits attained through design techniques aimed at reducing rotor/stator interaction noise levels. Many investigations have attempted to eliminate the excess noise in ground based facilities.⁸⁻¹⁴ These attempts have realized varying degrees of success.

An approach to simulating flight conditions is through the use of an anechoic wind tunnel. To this end the NASA Lewis 9- \times 15-ft low-speed wind tunnel has been modified to achieve near anechoic or freefield properties in the test section. The capabilities and limitations of the facility are described in Refs. 1, 15, and 16. Reference 1, in particular, concludes that the anechoic wind tunnel is a useful facility for applied research on aircraft engine fan noise during flight.

The purpose of this paper is to present representative model fan noise data indicating the type of acoustic information that can be obtained in the NASA Lewis anechoic wind tunnel. The model fan used for the test is designed to have the blade-passage tone cutoff below 107% of the design rotational speed.^{1,17-19} Where applicable, the results of the test are related to known forward flight effects and to the rotor/stator cutoff theory.^{17,18}

One-third octave band and narrowband spectra as well as continuous directivity patterns radiated from an inlet are presented. Data are shown over a range of conditions. The fan operating conditions varied include the rotational speed from 79 to 116% of the design value and the nozzle exit area. The ranges of wind-tunnel airflow velocities and inlet angle of attack are zero to 43 m/sec and zero to 30 deg, respectively.

Apparatus

Anechoic Wind Tunnel

Figure 1 is a schematic representation of the NASA Lewis 8- \times 6-ft²⁰ and 9- \times 15-ft wind tunnels.²¹ The NASA Lewis anechoic wind tunnel is the terminology used to refer to the combination of the 9- \times 15-ft low-speed test section, the

tunnel drive motors, and enclosed flow path. This facility has been used in the past for reverberant noise measurements as discussed in Refs. 15 and 22-30. More recently, however, the wind tunnel has been modified to allow anechoic experimentation in the acoustic direct field within the test section during tunnel operation.

The low-speed test section has been used extensively for aerodynamic testing, and its aerodynamic properties are reported in Ref. 21. That report indicates that the test-section velocity profile is uniform and the turbulence low. The flow being driven by the compressor circulates in a counter-clockwise direction making two 90-deg turns prior to reaching the 9- \times 15-ft test section. The airflow in the test section is varied by control of both the tunnel drive motor speed and the position of the flow-control doors immediately upstream of the test section (Fig. 1). Velocities in the range 10-70 m/sec are established and controlled in this manner. Airflow velocities below 10 m/sec may be induced by the use of auxiliary fans that are normally used for air circulation during air dryer reactivation operations.

Since the original construction, the test section has been modified by the addition of acoustic treatment on the test section walls, floor, and ceiling. The modification of the wind tunnel and the acoustic characteristics of the test section are reported in Refs. 1, 15, and 16. These reports indicate that anechoic or freefield properties exist for frequencies above 1000 Hz. For the purposes of acoustic testing, the entire anechoic wind tunnel has the favorable characteristics of remote drive motors, an acoustic muffler between the compressor and test section, and acoustic treatment on the first turn upstream and downstream of the test section (Fig. 1). With these features, the background noise level (one-third octave band) in the test section is 83 dB at 1000 Hz for a 40 m/sec airflow velocity. The background noise level is lower at

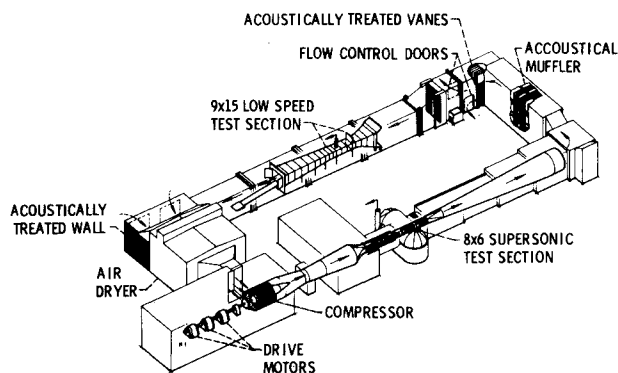


Fig. 1 The NASA Lewis 8- \times 6-ft and 9- \times 15-ft wind tunnels.

Received Jan. 18, 1977; presented as Paper 77-59 at the AIAA 15th Aerospace Sciences Meeting, Los Angeles, Calif., Jan 24-26, 1977; revision received June 13, 1977.

Index categories: Aeroacoustics; Airbreathing Propulsion; Noise.

*Aerospace Research Engineer, Wind Tunnel and Flight Division. Member AIAA.

†Aerospace Research Engineer, V/STOL and Noise Division. Member AIAA.

lower airflow velocities and at higher frequencies.¹⁶ As may be expected, the narrowband (25-Hz bandwidth) background level above 1000 Hz is at least 10 dB lower than the one-third octave background noise level.

Model Fan and Inlet

The model fan has 15 blades and a diameter of 50.8 cm. The design rotational speed is 8020 rpm, which results in a blade-passage tone of 2005 Hz. Throughout this paper, the fan rotational speed is expressed in terms of the percentage of the design rotational speed. The aerodynamic performance of the fan (using 11 stator vanes) is reported in Ref. 31. Reference 32 indicates that the aerodynamic characteristics of the 25-vane configuration used for the present tests are the same as the 11-stator-vane configuration. The rotor-stator spacing is approximately one rotor chord. The fan could be operated to a maximum of 120% of the design rotational speed. At this rotational speed, the fan-pressure ratio is approximately 1.25 and the rotor-tip speed 256 m/sec. This model is therefore representative of a fan having a low fan pressure ratio and subsonic tip speed.

Some of the acoustic design properties of the fan are discussed in Ref. 1. Of particular importance to this paper are the tone cutoff properties as described in Refs. 17 and 18. For this model fan, which has a stator-vane/rotor-blade ratio of 1.67, the cutoff theory predicts that the fundamental or first harmonic of the blade passage tone will not propagate below 107% of the design speed. This feature of the fan does not consider any effect due to the inlet radius contraction as reported in Ref. 33. According to the cutoff theory, the second harmonic tone will propagate at all fan rotational speeds. Propagation of the second harmonic is discussed in Ref. 1 and may be expected to exhibit a distinctively lobed pattern when not masked by extraneous noise sources.

The inlet used during this test is representative of a conventional flight inlet having a low throat Mach number (0.60). The inlet lip geometry is a 2:1 ellipse with an area contraction ratio (highlight-to-throat) of 1.46. The inlet provides very little flow diffusion with a fan-annulus(diffuser exit)-to-throat area ratio of 1.011. Even though the inlet flow diffusion is low, there is an inlet radius contraction at the throat that compensates for the centerbody of the fan. The ratio of inlet-throat-to-fan-tip radii is 0.883. The inlet aerodynamic performance is reported in Ref. 32. At the conditions discussed in this paper, the inlet flow is always attached. The inlet-total-pressure recovery is always above 0.99 and total-pressure distortion (maximum minus minimum/average) below 0.02.

The installation of the fan and inlet in the anechoic wind tunnel is shown in Fig. 2. The fan and drive turbine discharge flows are ducted away and turned 90 deg, pass through an

acoustic muffler, and are exhausted outside the test section.³² An adjustable plug at the muffler exit allows the remote setting of the nozzle area and thereby the fan operating point. The 90-deg elbow and vertical duct are lined with acoustic treatment to suppress aft fan noise. In addition, the turning vanes in the elbow are acoustically treated to prevent reflection of the aft fan noise upstream. As shown in Fig. 2, inlet angle of attack is varied by rotating the model in the horizontal plane.

Acoustic Instrumentation

The primary piece of acoustic instrumentation is also shown in Fig. 2 and consists of a "sword" microphone and rotating microphone boom. The sword microphone system employs a standard commercially available microphone head (0.635 cm diam) with bullet nose. The unique feature of the system is the remote location of the cathode follower, which is located in the thickened (vane) portion of the support. This feature allows a very thin, streamlined microphone system that weathervanes above its support. This is done so that the microphone is always oriented directly into the airflow which is the condition of minimum wind noise on the microphone.

The microphone is located 3.6 fan diameters from the intersection of the fan axis with the inlet highlight plane. It is mounted on the end of a boom that is capable of being rotated about a vertical axis through the inlet face. By rotating the boom, the microphone can be swept in a circular arc in the horizontal plane at the height of the fan axis.

The electrical signal from the microphone is treated in a conventional manner and recorded on magnetic tape. In addition, the microphone signal is processed through additional amplifiers, filters, and logarithmic converters to yield an on-line (real-time) analysis of the acoustic signature. This system provides an on-line plot of the inlet directivity pattern as the microphone boom is remotely rotated.

Test Matrix

Basically the tests were performed over variations in four parameters: wind-tunnel airflow velocity, model fan rotational speed, fan nozzle area, and inlet angle of attack. A fan map which shows the fan operating conditions is presented in Fig. 3. As indicated, the data were obtained along either a fixed operating line (fixed nozzle area for 43 m/sec tunnel velocity) or a fixed rotational speed line.

Along the fixed operating line (circular symbols, Fig. 3), the fan corrected rotational speed was set at 79, 95, 103, 106, 110, and 116% of the design speed. For all of these rotational speeds, data were obtained at wind-tunnel airflow velocities of 0, 8, and 43 m/sec and an angle of attack of 0 deg. For the two rotational speeds of 95 and 116% of design, additional zero-angle-of-attack data were obtained at wind-tunnel

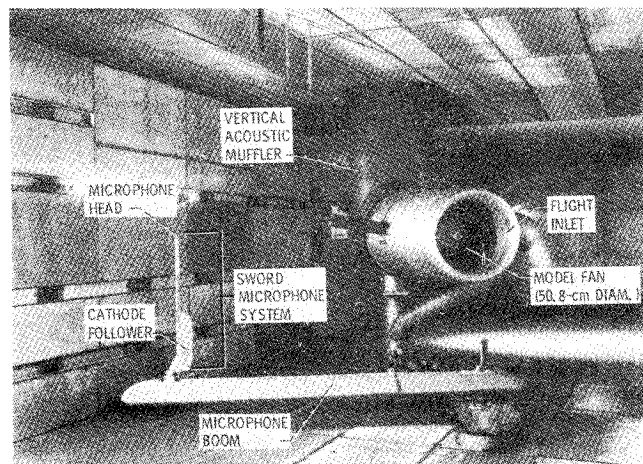


Fig. 2 Model fan installed in the anechoic wind tunnel.

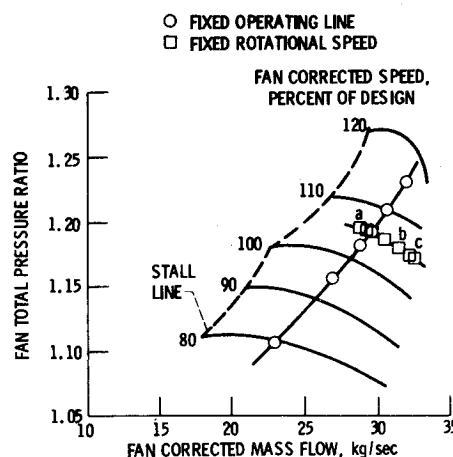


Fig. 3 Performance map for the model fan.

airflow velocities of 14, 22, and 32 m/sec. For a selected airflow velocity of 43 m/sec, data were obtained at angles of attack of 15 and 30 deg for the 95 and 116% design speed conditions.

An alternate method of setting the fan operating condition was along a fixed-rotational-speed line (square symbols, Fig. 3). For a fixed rotational speed of 106% of design, the fan nozzle area was varied to set the operating condition. This was done at a tunnel velocity of 43 m/sec and 0-deg angle of attack only.

Test Procedure

For each model fan operating condition in the test matrix, the individual conditions were established sequentially in the following order: 1) wind-tunnel airflow velocity, 2) fan rotational speed, 3) fan mass flow (by adjusting the nozzle area), and 4) inlet angle of attack. Once the desired model operating condition was established, data were obtained with the microphone sweeping a circular arc, the microphone fixed at specified locations, and finally again with the microphone sweeping.

Initially, the microphone was set at a shallow microphone angle (20 deg for 0-deg angle of attack, and 35 deg for nonzero angles of attack). The microphone angle[†] was measured with respect to the fan axis in all cases. The microphone angle was then varied at 2.5 deg/sec to 120 deg and returned to the initial angle. During the first sweep and return, the one-third octave band sound pressure level was recorded on-line at the frequencies containing the first and second harmonics of the blade passage tone. Data were obtained during both the initial and return sweeps to assure repeatability. After completing the microphone sweep, the microphone was rotated to fixed positions of 30, 60, and finally 90 deg (60 and 90 deg only for nonzero angles of attack). The unfiltered microphone signal was then recorded on magnetic tape for 1 min at each fixed position. These data were used later for one-third octave band and narrowband spectral analysis. Finally, the microphone was again swept a second time in the same manner as described above. In this case, the one-third octave band sound pressure level was recorded on-line at two nonintegral-multiple frequencies (either 0.7 and 1.4 or 1.5 and 2.5) of the blade passage tone.

Results

This section presents representative examples of the data obtained. Figures 4, 5, and 6 show typical data for the on-line directivity traces, one-third octave band spectra, and narrowband spectra, respectively. These figures are described briefly here and in more detail in the Discussion of the Results.

On-Line Data

Figure 4 contains examples of the directivity patterns obtained from the on-line acoustic measurements for a rotational speed of 95% of design and 0-deg angle of attack. Figure 4a contains data obtained under static (no wind-tunnel airflow) conditions, whereas Fig. 4b illustrates the results at an airflow velocity of 43 m/sec. The ordinate in each case is the one-third octave band sound pressure level, whereas the abscissa is the microphone angle measured with respect to the fan axis. Data are shown for one-third octave band center frequencies of 1, 2, 0.7, and 1.4 multiples of the blade passage tone, and the range of microphone angles is 20–120 deg.

One-Third Octave Band Spectra

The data recorded with the microphone in a fixed location were processed on a one-third octave band analyzer using a 4-

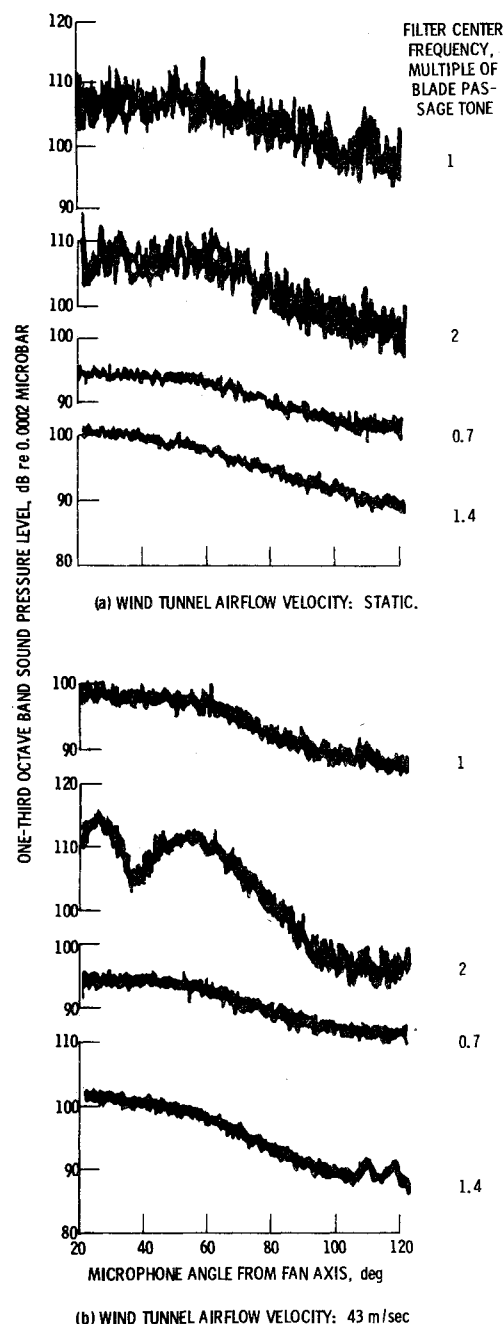


Fig. 4 Sound pressure level directivity: fan rotational speed—95% of design; inlet angle of attack—0 deg.

sec integration time. Figure 5 shows one-third octave band sound pressure level spectra from 1000 to 20,000 Hz for rotational speeds of 79, 95, 106, and 116% of the design speed. The data are shown for 0-deg angle of attack, for static and 43 m/sec airflow velocity, and for microphone angles of 30, 60, and 90 deg.

Narrowband Spectra

In the same manner as the one-third octave band analysis, the fixed microphone data were processed by the use of a narrow-band (25 Hz bandwidth) analyzer with an approximate integration time of 11 sec. Figure 6 shows the narrowband sound pressure level spectra, up to 10,000 Hz, for rotational speed of 79, 95, 106, and 116% of the design speed. The data are shown for 0-deg angle of attack, for static and 43 m/sec airflow velocity, and for a microphone angle of 60 deg to the fan axis.

[†]For nonzero angles of attack, the microphone angles over which the data are obtained are representative of the forward quadrant below the inlet, which, in the case of an aircraft, is the region of interest to a ground observer.

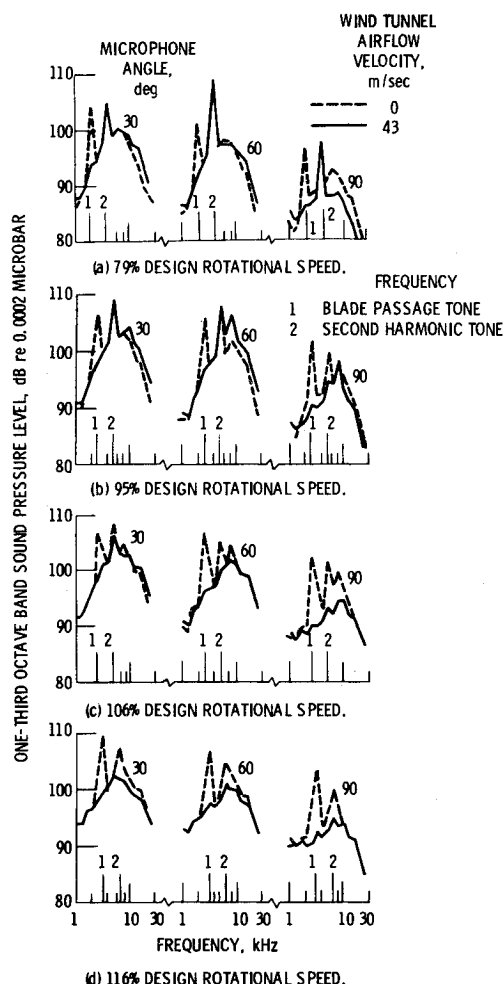


Fig. 5 One-third octave band sound pressure level spectra: inlet angle of attack—0 deg.

Discussion of the Results

The discussion of the results of this test program is divided into four categories: 1) the effect due to forward velocity, 2) the effect due to fan rotational speed, 3) the effect of fan blade loading, and 4) the effect of inlet angle of attack. It should be kept in mind that the effects enumerated above are in many instances interrelated.

Forward Velocity

One of the effects of airplane forward flight on the engine acoustic signature is the large reduction in tone unsteadiness, as discussed in Ref. 1. The examples of the on-line traces (Fig. 4) indicate this same effect when the data at the static and 43 m/sec airflow conditions are compared. The traces of the first and second harmonics of the blade passage tone show significant reductions in tone unsteadiness (peak-to-valley variation of the trace at any given microphone angle) under wind-tunnel flow conditions and become similar in unsteadiness to the broadband noise.

The variation of tone unsteadiness with wind-tunnel airflow is shown quantitatively in Fig. 7 for 0-deg angle of attack, 95% fan rotational speed, and a 60-deg microphone angle. A measure of the tone unsteadiness is taken to be the maximum peak-to-valley variation in the one-third octave band sound pressure level over a time period of approximately 10 sec. The unsteadiness of the first and second harmonics of the blade passage tone in decibels is plotted as a function of wind-tunnel airflow velocity in meters per second. The inset traces on the figure are representative of the acoustic signatures over a 4-sec time interval for wind tunnel airflow velocities of zero and 43 m/sec.

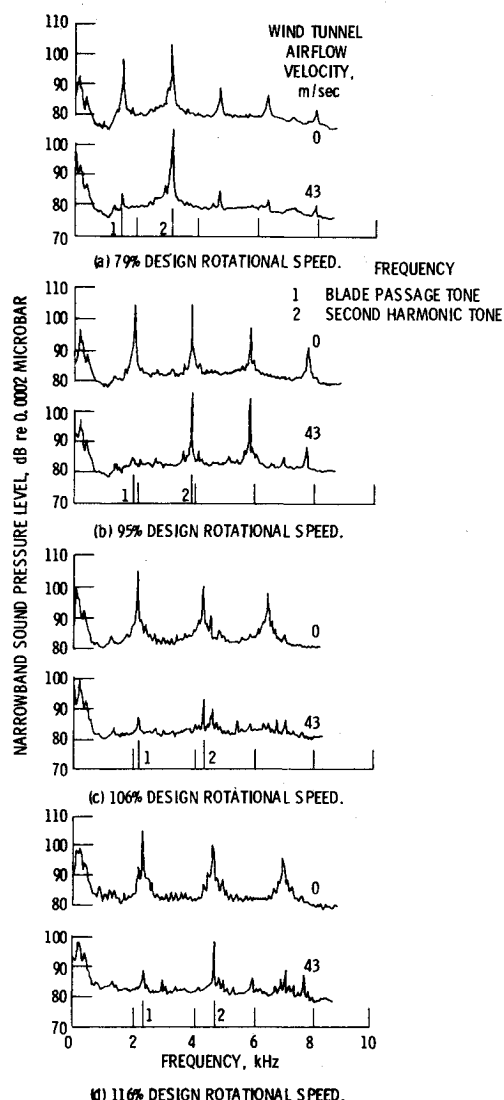


Fig. 6 Narrowband sound pressure level spectra: inlet angle of attack—0 deg; microphone angle—60 deg.

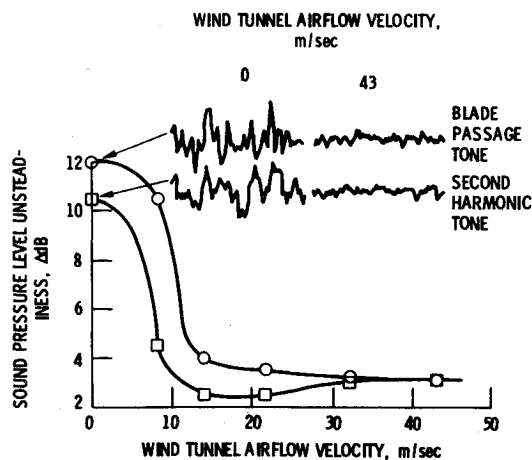


Fig. 7 Effect of forward velocity on tone unsteadiness at 95% design speed; microphone angle—60 deg; inlet angle of attack—0 deg.

Under static wind-tunnel conditions, the sound-pressure level unsteadiness of each of the tones is more than 10 dB. At 43-m/sec airflow velocity, the unsteadiness is approximately 3 dB. The decrease in unsteadiness with increasing airflow velocity is abrupt with the reduction in unsteadiness being essentially complete by 15 m/sec. It will be shown in the next

section that the airflow velocity at which this transition is complete is not always 15 m/sec but is dependent on the model operating conditions.

In addition to the reduction in unsteadiness discussed above, comparison of Figs. 4a and b also shows a large reduction in the sound pressure level of the blade passage tone between the static and wind-tunnel flow cases. As an example, the blade passage tone level is approximately 107 dB statically and 98 dB with tunnel flow at a microphone angle of 20 deg. This effect is expected, since the fan is designed to have the blade passage tone cutoff at rotational speeds below the design speed. When the cutoff condition is realized, a blade passage tone is not generated. This design feature in a subsonic-tip-speed fan has not been directly demonstrated in static test facilities because of a rotor-alone blade passage tone, which is generated by the interaction of the fan with the inflow turbulence.⁵

All the parts of Figs. 5 and 6 also indicate a large reduction in the sound pressure level of the blade passage tone once the tunnel flow is established. These figures also indicate the presence of a strong second harmonic of the blade passage tone, which at low fan rotational speeds is relatively unaffected by forward velocity.

Figures 8 and 9 show the effect of forward velocity at 0-deg angle of attack much more directly. On both figures, the sound pressure levels of the first and second harmonics of the blade passage tone are shown as a function of airflow velocity. The tone levels are determined from the narrowband spectra at the fixed microphone angles of 30, 60, and 90 deg as indicated. Figure 8 represents the data obtained at a rotational speed of 95% of design, whereas Fig. 9 shows the data at a speed of 116% of design.

Figure 8 indicates a monotonic decrease of as much as 20 dB in the sound pressure level of the blade passage tone between zero and 15 m/sec. The level is unchanged above 15 m/sec. This result suggests that the inflow turbulence present at the static condition, which causes rotor-alone noise is absent above an airflow of 15 m/sec. The sound pressure level of the second harmonic tone is not cut off and therefore is comparatively unchanged in level due to forward velocity.

Figure 9 indicates much the same situation for the higher rotational speed as that of the low rotational speed (Fig. 8). However, the full effect of forward velocity in this case may not be realized until the airflow velocity is 20 m/sec. This result may well be due to the detailed nature of the turbulence present in the test section at static and near-static conditions. However, an alternate possibility exists for the present wind-tunnel model installation (Fig. 2). The closest obstacle ex-

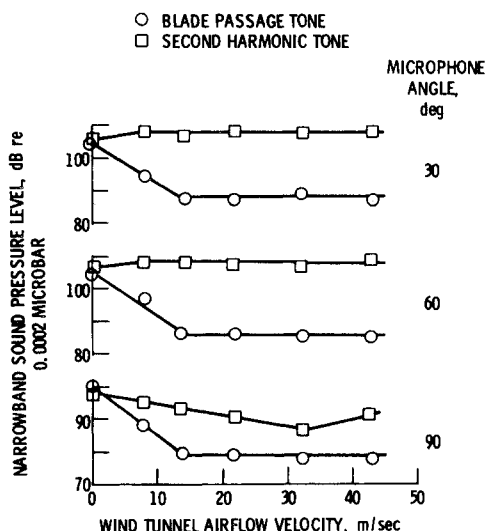


Fig. 8 Effect of forward velocity on sound pressure level at 95% design speed: inlet angle of attack—0 deg.

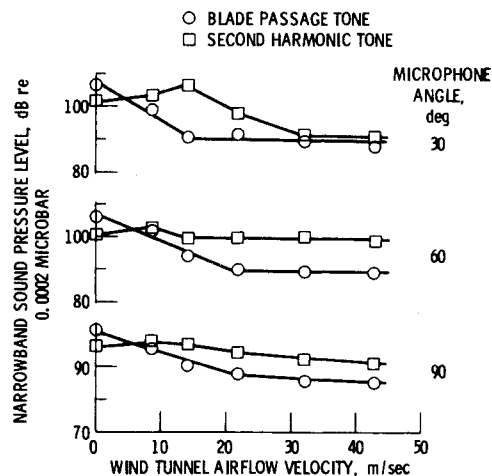


Fig. 9 Effect of forward velocity on sound-pressure level at 116% design speed: inlet angle of attack—0 deg.

ternal to the fan that may be the cause of an inflow turbulence is the microphone boom. Such inflow turbulence would cause an increase in the sound pressure level of the blade passage tone. To avoid ingestion of the turbulence caused by the microphone boom the capture streamtube of the inlet flow must be small enough to exclude the boom. For a given mass flow (rotational speed), the size of the capture streamtube decreases with increasing tunnel velocity. Thus, below some tunnel velocity the boom turbulence could enter the inlet and cause a blade passage tone, whereas above that tunnel velocity the boom turbulence would not enter the inlet, and the blade passage tone may be absent. This is consistent with data shown in Figs. 8 and 9. Furthermore, the size of the capture streamtube increases with increasing fan mass flow so at higher fan mass flows the tunnel velocity must be greater to keep the capture streamtube small enough to exclude the boom. This is consistent with the higher tunnel velocity at which full blade passage tone reduction is realized at the higher fan speed (Fig. 9, compared with Fig. 8). Finally, if the boom had not been used during the test, the complete effect of forward velocity might have been realized at a tunnel airflow velocity less than 15 m/sec.

Rotational Speed

The most significant effect to be expected due to a change in rotational speed is the change in the acoustic signatures as predicted by the cutoff theory. In particular, at low rotational speeds the blade passage tone is cut off and the second harmonic tone is cut on. At high rotational speeds, both the first and second harmonics should be cut on. According to the previous discussion, the effect can be observed only with tunnel velocity.

The absence of a blade passage tone at low rotational speeds is shown in Figs. 4, 5a and b and 6a and b. In particular, the narrowband spectrum of Fig. 6b indicates a nearly complete absence of a blade passage tone. These observations verify the predictions of the cutoff theory.

Another feature of the data of Fig. 4b is the distinctive lobular directivity pattern of the second harmonic of the blade passage tone. It is notable that this lobular directivity pattern is not exposed until the forward velocity effect is realized as can be seen by comparing the data of Fig. 4a and b. The pattern of Fig. 4b is characteristic of the spatial pattern that can be generated by a cut on rotor/stator interaction. Evidence of these patterns is also shown in Ref. 19. This result coupled with the fact that the directionality of the noise at the blade passage frequency (Fig. 4b) has the same basic pattern as that of broadband noise implies that the blade passage tone is cut off and the second harmonic cut on at rotational speeds below the design rotational speed.

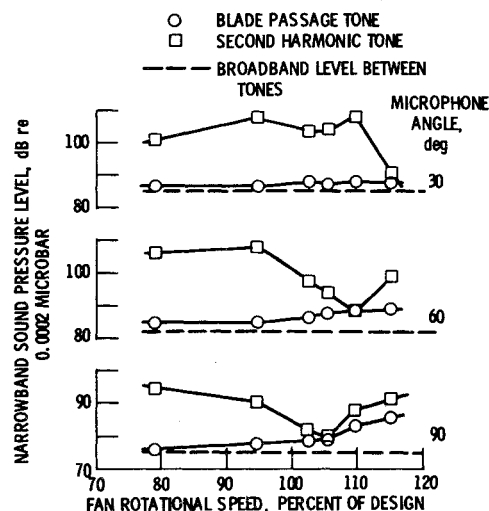


Fig. 10 Effect of fan rotational speed on sound pressure level at a tunnel velocity of 43 m/sec; inlet angle of attack—0 deg.

The data obtained during this test can also be used to determine if the blade passage tone is cut on at rotational speeds above design. Using Refs. 17 and 18, the blade passage tone should be cut on at and above rotational speeds of 107% of the design value. However, Ref. 33 states that because of the effect of the inlet radius contraction the cut on condition forward of the inlet is not realized until a higher rotational speed. Once the blade passage tone is cut on, the sound pressure level of the tone should increase with respect to both the broadband level and the level of the second harmonic. This effect should first become evident at the microphone position of 90 deg to the fan axis.

An indication of a weak blade passage tone at 116% fan speed is shown in Fig. 5d at the 90-deg microphone angle and in Fig. 6d. Figure 10 presents some further information about the nature of the acoustic signatures at a wind-tunnel airflow velocity of 43 m/sec and 0-deg inlet angle of attack. In Fig. 10, the sound pressure levels of the first and second harmonics of the blade passage tone are shown as a function of rotational speed. The sound pressure levels are determined from the narrowband spectra for the fixed microphone positions of 30, 60 and 90 deg.

The data of Fig. 10 show several features. First, the blade passage tone does not increase dramatically with increasing fan rotational speed as one might expect. A small increase in the blade passage tone level (with respect to the second harmonic tone and broadband levels) is observed, however, at the 60- and 90-deg microphone angles. An increase in tone level due to cuton would be expected as noted previously to be first observed at high microphone angles, as in Fig. 10. The lack of a dramatic increase in the blade passage tone may be due in part to the inlet radius contraction,³³ and a more detailed study of the inlet-fan combination is required. Second, at particular microphone angles and fan speeds the second harmonic tone level decreases to the value of the blade passage tone level and close to that of the broadband level. These low values of the second harmonic tone level may be associated with a minimum in the lobular directivity patterns such as those evident in Fig. 4b.

Blade Loading

The fan map (Fig. 3) shows the various fan operating points for which data were obtained at a constant rotational speed. By varying the nozzle area while maintaining a rotational speed of 106% of the design value, various conditions of fan mass flow and fan pressure ratio are established. These changes result in significant differences in the fan blade loading and the duct Mach number. The fan blade loading parameter used in this paper is the ratio of the total pressure

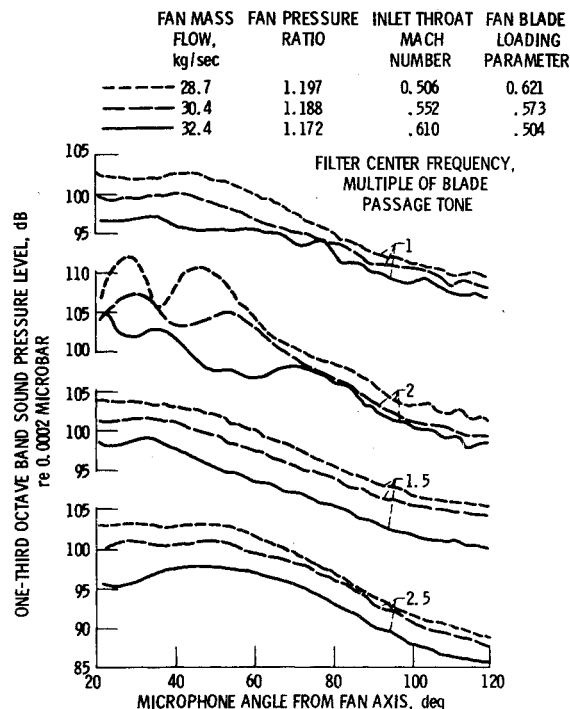


Fig. 11 Effect of fan blade loading directivity at a tunnel velocity of 43 m/sec and 106% design speed; angle of attack—0 deg.

rise across the fan and the flow dynamic pressure relative to the blade at the tip of the fan. The values of the above parameters are presented in the table in Fig. 11.

The curves of Fig. 11 show the resulting acoustic directivity patterns of the tones and broadband noise for the two extreme conditions on the speed line and one intermediate case (points a, b, and c on Fig. 3) for a wind-tunnel airflow velocity of 43 m/sec and 0-deg angle of attack. The curves shown on Fig. 11 are obtained from the on-line directivity traces of the one-third octave band sound pressure level as illustrated in Fig. 4. In general, there is an increase in both the tone and broadband sound pressure levels with increased blade loading; that is, as the fan weight flow is reduced and the fan pressure ratio is increased. This effect agrees with other results that have shown an increase in noise level with increased blade loading.^{34,35} In addition, there is a large effect on the directivity pattern of the second harmonic of the blade passage tone as the blade loading is increased. Between microphone angles of 20 and 70 deg, there is a lobular directivity pattern that becomes increasingly distinct.

Angle of Attack

The effect that inlet angle of attack can have on inlet acoustic directivity is shown in Fig. 12 for an airflow velocity of 43 m/sec and a fan rotational speed of 95%. The figure is constructed in the same manner as Figs. 4 and 11 with directivity patterns shown for angle of attack of 0, 15, and 30 deg. Clearly in this particular example there is an increase in the sound pressure level of the blade passage tone and broadband noise as the angle of attack is increased. The inlet angle of attack also has a very large effect on the second harmonic tone. Any increase in sound power level is difficult to identify, but there is a significant shift in the directionality pattern of the sound pressure level. The change in the angle of maximum sound pressure level of the directivity pattern is particularly important to the case of an aircraft because both the level and angular direction (with respect to the aircraft) of the maximum perceived noise on the ground can be affected.

Angle of attack can affect the noise in several ways. First, the nonuniform velocity profile at the inlet face when the inlet is at a nonzero or upward angle of attack can cause the noise

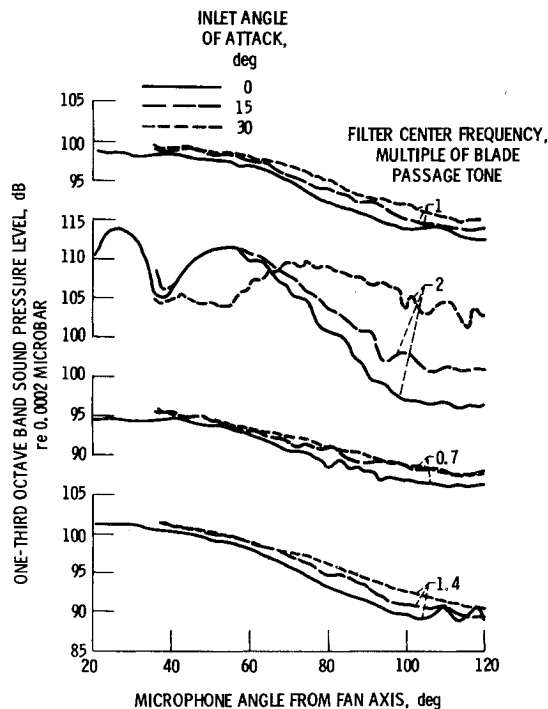


Fig. 12 Effect of angle of attack on directivity at a tunnel velocity of 43 m/sec and 95% design speed.

to be refracted downward. Second, any modification or nonuniformity of the flow at the fan face including the boundary layer can change the character and increase the level of the generated noise. Either or both of these angle-of-attack effects could cause the observed changes in level and directionality. The changes in the sound pressure level or acoustic patterns cannot be attributed to an inlet flow separation, since Ref. 32 has shown that the flow remains attached over these ranges of angle of attack and fan mass flow.

Summary of Results

The acoustic signatures of a model fan in the NASA Lewis anechoic wind tunnel are discussed. The model fan is designed to have the blade passage tone cut off for rotational speeds below 107% of the design speed. The data presented are one-third octave band and narrowband spectra and continuous on-line traces of the directivity patterns radiated from an inlet over ranges of fan operating conditions, wind-tunnel airflow velocity, and inlet angle of attack. The major results of this paper may be summarized as follows:

1) Presence of a wind-tunnel flow velocity greater than approximately 20 m/sec results in a large reduction in both the unsteadiness and the sound pressure level of the blade passage tone compared to the static (no wind-tunnel airflow) condition.

2) The airflow velocity at which the full forward velocity effect is achieved is related to the amount of flow through the inlet and the location of any flow-disturbing device external to the inlet.

3) The cutoff design feature of the model fan is revealed by the absence of a blade passage tone and the distinctive lobular acoustic directivity pattern of the second harmonic of the blade passage tone at forward velocity conditions.

4) Changes in the fan weight flow, fan pressure ratio, fan blade loading, or inlet angle of attack strongly affect the acoustic signatures.

5) It is difficult to isolate the effects of the various fan and wind-tunnel operating conditions tested. As of this time, all aspects of the acoustic signatures have not been explained entirely by the effects of inflow turbulence (rotor-alone noise) and rotor/stator interaction noise. A more detailed study of

the acoustic characteristics of this fan/inlet combination is required.

References

- Heidmann, M.F. and Dietrich, D.A., "Simulation of Flight-Type Engine Fan Noise in the NASA-Lewis 9 x 15 Anechoic Wind Tunnel," NASA TM X-73540, 1976.
- Povinelli, F.P., Dittmar, J.H., and Woodward, R.P., "Effects of Installation Caused Flow Distortion on Noise from a Fan Designed for Turbofan Engines," NASA TN D-7076, 1972.
- Hanson, D.B., "A Study of Subsonic Fan Noise Sources," AIAA Paper 75-468, Hampton, Va., 1975.
- Hansen, D.G., "Spectrum of Rotor Noise Caused by Atmospheric Turbulence," *Journal of the Acoustical Society of America*, Vol. 55 (Supplement), Spring 1974, pp. S3-S4.
- Heidmann, M.F., "An Observation on Tone Cut-Off in Static Test Data From Jet Engine Fans," NASA TM X-3296, 1975.
- Merriman, J.E. and Good, R.C., "Effect of Forward Motion on Fan Noise," AIAA Paper 75-464, Hampton, Va., 1975.
- Pickett, G.F., "Effects of Non-Uniform Inflow on Fan Noise," presented at the 87th Acoustical Society of America Meeting, New York, April 1974.
- Cumsty, M.A. and Lowrie, B.W., "The Cause of Tone Generation by Aero-Engine Fans at High Subsonic Tip Speeds and the Effect of Forward Speed," ASME Paper 73-WA/GT-4, Detroit, Mich., 1973.
- Roundhill, J.P. and Schaut, L.A., "Model and Full-Scale Test Results Relating to Fan-Noise In-Flight Effects," AIAA Paper 75-465, Hampton, Va., 1975.
- Lowrie, B.W., "Simulation of Flight Effects on Aero Engine Fan Noise," AIAA Paper 75-463, Hampton, Va., 1975.
- Hodder, B.K., "The Effects of Forward Speed on Fan Inlet Turbulence and Its Relation to Tone Noise Generation," NASA TM X-62381, 1974.
- Hodder, B.K., "An Investigation of Possible Causes for the Reduction of Fan Noise in Flight," AIAA Paper 76-585, Palo Alto, Calif., 1976.
- Hodder, B.K., "Investigation of the Effect of Inlet Turbulence Length Scale on Fan Discrete Tone Noise," NASA TM X-62300, 1973.
- Feiler, C.E. and Merriman, J.E., "Effects of Forward Velocity and Acoustic Treatment on Inlet Fan Noise," AIAA Paper 74-946, Los Angeles, Calif., 1974.
- Diedrich, J.H. and Luidens, R.W., "Measurement of Model Propulsion System Noise in a Low-Speed Wind Tunnel," AIAA Paper 76-91, Washington, D.C., 1976.
- Rentz, P.E., "Softwall Acoustical Characteristics and Measurement Capabilities of the NASA-Lewis 9 x 15 Foot Low Speed Wind Tunnel," NASA CR-135026, 1976.
- Tyler, J.M. and Sofrin, T.G., "Axial Flow Compressor Noise Studies," *SAE Transactions*, Vol. 70, 1962, pp. 309-332; also SAE paper 345D, April 1961.
- Sofrin, T.G. and McCann, J.C., "Pratt and Whitney Aircraft Experience in Compressor-Noise Reduction," *Journal of the Acoustical Society of America*, Vol. 40, Nov. 1966, pp. 1248-1249.
- Cumpsty, N.A., "Tone Noise from Rotor/Stator Interactions in High Speed Fans," *Journal of Sound and Vibration*, Vol. 24, Oct. 1972, pp. 393-409.
- Swallow, R.J. and Aiello, R.A., "NASA-Lewis 8- by 6-Foot Supersonic Wind Tunnel Facility Description with Performance Data," NASA TM X-71542, 1974.
- Yuska, J.A., Diedrich, J.H., and Clough, N., "Lewis 9- by 15-Foot V/STOL Wind Tunnel," NASA TM X-2305, 1971.
- Loeffler, I.J., Lieblein, S., and Stockman, N.O., "Effect of Rotor Design Tip Speed on Noise of a 1.21 Pressure Ratio Model Fan Under Static Conditions," ASME Paper 73-WA/GT-11, Detroit, Mich., 1973.
- Piersol, A.G. and Rentz, P.E., "Utilization and Enhancement of the NASA-Lewis 9 x 15 Foot V/STOL Wind Tunnel for Inlet Noise Research," Bolt, Beranek, and Newman, Inc., Cambridge, Mass., BBN-2743, May 1974.
- Wesoky, H.L., Abbot, J.M., Albers, J.A., and Dietrich, D.A., "Low-Speed Wind Tunnel Tests of a 50.8 cm. (20-in.) 1.15-Pressure-Ratio Fan Engine Model," NASA TM X-3062, 1974.
- Miller, B.A. and Abbott, J.M., "Aerodynamic and Acoustic Performance of Two Choked-Flow Inlets Under Static Conditions," NASA TM X-2629, 1972.
- Miller, B.A. and Abbott, J.M., "Low-Speed Wind-Tunnel Investigation of the Aerodynamic and Acoustic Performance of a

Translating-Centerbody Choked Flow Inlet," NASA TM X-2773, 1973.

²⁷ Abbott, J.M., Miller, B.A., and Golladay, R.L., "Low-Speed Wind-Tunnel Investigation of the Aerodynamic and Acoustic Performance of a Translating-Grid Choked-Flow Inlet," NASA TM X-2966, 1974.

²⁸ Miller, B.A., Dastoli, B.J., and Wesoky, H.L., "Effect of Entry-Lip Design on Aerodynamics and Acoustics of High-Throat-Mach-Number Inlets for the Quiet, Clean, Short-Haul Experimental Engine," NASA TM X-3222, 1975.

²⁹ Abbott, J.M., "Aeroacoustic Performance of Scale Model Sonic Inlets," AIAA Paper 75-202, Pasadena, Calif., 1975.

³⁰ Rentz, P.E., "Hardwall Acoustical Characteristics and Measurement Capabilities of the NASA-Lewis 9 x 15 Low Speed Wind Tunnel," NASA CR-135025, 1976.

³¹ Lewis, G.W. Jr. and Tysl, E.R., "Overall and Blade-Element Performance of a 1.20-Pressure-Ratio Fan Stage at Design Blade Setting Angle," NASA TM X-3101, 1974.

³² Abbott, J.M., Diedrich, J.H., and Williams, R.C., "Low Speed Aerodynamic Performance of 50.8-Centimeter-Diameter Noise Suppressing Inlets for the Quiet, Clean, Short-Haul Experimental Engine (QCSEE)," to be published as a NASA TM X.

³³ Mathews, D.C. and Nagel, R.T., "Inlet Geometry and Axial Mach Number Effects on Fan Noise Propagation," AIAA Paper 73-1022, Seattle, Wash., 1973.

³⁴ Feiler, C.E. and Conrad, W., "Noise from Turbomachinery," AIAA Paper 73-815, St. Louis, Mo., 1973.

³⁵ Heidmann, M.F. and Feiler, C.E., "Noise Comparisons From Full-Scale Fan Tests at NASA-Lewis Research Center," AIAA Paper 73-1017, Seattle, Wash., 1973.

From the AIAA Progress in Astronautics and Aeronautics Series . . .

AEROACOUSTICS: FAN, STOL, AND BOUNDARY LAYER NOISE; SONIC BOOM; AEROACOUSTIC INSTRUMENTATION—v. 38

Edited by Henry T. Nagamatsu, General Electric Research and Development Center; Jack V. O'Keefe, The Boeing Company; and Ira R. Schwartz, NASA Ames Development Center

A companion to Aeroacoustics: Jet and Combustion Noise; Duct Acoustics, volume 37 in the series.

Twenty-nine papers, with summaries of panel discussions, comprise this volume, covering fan noise, STOL and rotor noise, acoustics of boundary layers and structural response, broadband noise generation, airfoil-wake interactions, blade spacing, supersonic fans, and inlet geometry. Studies of STOL and rotor noise cover mechanisms and prediction, suppression, spectral trends, and an engine-over-the-wing concept. Structural phenomena include panel response, high-temperature fatigue, and reentry vehicle loads, and boundary layer studies examine attached and separated turbulent pressure fluctuations, supersonic and hypersonic.

Sonic boom studies examine high-altitude overpressure, space shuttle boom, a low-boom supersonic transport, shock wave distortion, nonlinear acoustics, and far-field effects. Instrumentation includes directional microphone, jet flow source location, various sensors, shear flow measurement, laser velocimeters, and comparisons of wind tunnel and flight test data.

509 pp. 6 x 9, illus. \$19.00 Mem. \$30.00 List

TO ORDER WRITE: Publications Dept., AIAA, 1290 Avenue of the Americas, New York, N. Y. 10019